Low-Dimensional, Reduced Phases of Ultrathin TiO_2

Anthoula C. Papageorgiou, Chi L. Pang, Qiao Chen, and Geoff Thornton*

London Centre for Nanotechnology and Chemistry Department, University College London, 17-19 Gordon Street, London WC1H 0AH, U.K.

ARTICLE

ABSTRACT Reduced phases of ultrathin rutile TiO_2(110) grown on Ni(110) have been characterized with scanning tunneling microscopy and low-energy electron diffraction. Areas of 1×2 reconstruction are observed as well as {132} and {121} families of crystallographic shear planes. These phases are assigned by comparison with analogous phases on native rutile TiO_2(110).

KEYWORDS: ultrathin film · TiO_2 · rutile · crystallographic shear plane · self-assembly · facet · STM

Ultrathin oxides grown on metallic substrates are currently a subject of intensive study in the emerging field of nanoscience. Possible applications include utilizing the self-assembled, low-dimensional nanostuctures in electronic devices, nanocatalysts, and gas sensors. Controlling the oxidation state and the dimensions of these nanostructures may allow the production of a new range of technologically important materials.

Titanium dioxide nanostructures grown on Ni(110) have previously been studied with scanning tunneling microscopy (STM), low-energy electron diffraction (LEED), and soft X-ray photoelectron spectroscopy (SXPS).[1–3] It was shown that islands of rutile TiO_2(110) grow on top of a wetting layer that also has TiO_2 stoichiometry. Rutile islands, with heights of up to 40 Å, typically grow on the Ni(110) single crystal with the TiO_2 [1$\bar{1}$0] azimuth parallel to the Ni [001] direction. In addition, minority domains can be observed with the [001] direction of TiO_2(110) aligned parallel to the [001] direction of the substrate.[4] These islands are usually terminated by the unreconstructed TiO_2(110) 1×1 phase (Figure 1a) and are referred to as "rutile islands" in the rest of this article.

One of the key motivations for our current study is to establish to what extent the ultrathin titania mimics the behavior of the (110) surface of a rutile single crystal (henceforth referred to as the "native surface"). Differences might be expected because rutile TiO_2(110) is incommensurate with respect the Ni(110) substrate.

The 1×1-terminated native surface is usually prepared by sputtering with inert gas ions and annealing to about 700–1200 K. This results in reduction of the crystal and the introduction of n-type conductivity. When samples are annealed to higher temperatures or when they are heavily reduced, a 1×2 reconstruction appears.[5–19] On the basis of STM images, Onishi and Iwasawa[5] proposed an "added Ti_2O_3 row model" for the 1×2 reconstruction, shown in Figure 1b. This model has been shown to be consistent with a range of experimental results, such as quantitative LEED, as well as theoretical calculations.[6,10]

Magnéli phases have also been observed on native surfaces, through the formation of crystallographic shear (CS) planes.[15–23] A detailed review of CS plane formation in titanium oxides is given by Bursill and Hyde,[20] and the energetics of this system have been studied by Catlow and James.[24] CS plane formation is caused by reduction of the crystal. As the concentration of oxygen vacancies increases, they order into specific planes, resulting in the collapse of the crystal by a slip of half a unit cell along the CS planes. Arrays of (132) CS planes terminated at the TiO_2(110) surface are shown in Figure 2. Two different arrangements of these CS planes are illustrated.

The first arrangement consists of half-height steps where alternate CS planes slip half a unit cell up and then down. We refer to these as "up−down" steps. In the second arrangement all CS planes slip in the same direction, and we refer to this as a "stair -

*Address correspondence to g.thornton@ucl.ac.uk.

Received for review August 10, 2007 and accepted November 01, 2007.

Published online November 30, 2007.
10.1021/nn700158s CCC: $37.00

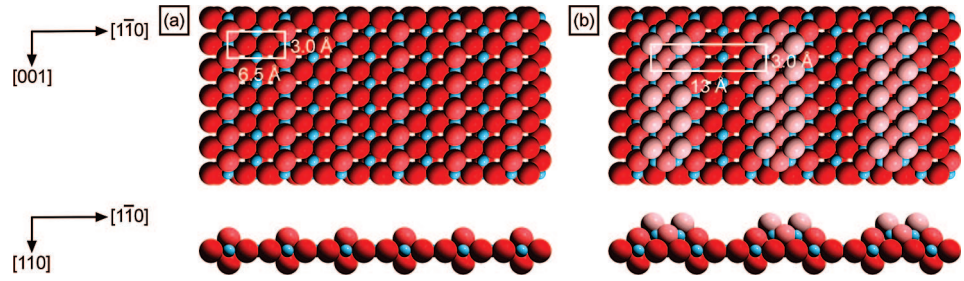

Figure 1. Atomic models of TiO_2(110) surfaces. The high-symmetry axes and the surface unit cells are indicated. Small blue spheres represent Ti atoms and larger red spheres O atoms. O atoms nearer to the surface are shaded lighter. (a) The unreconstructed TiO_2(110) 1×1 surface. (b) The proposed added Ti_2O_3 row model for the TiO_2(110) 1×2 reconstruction.[5]

case" arrangement of steps. In the up–down steps, the CS planes can be thought of as pairs comprising the *up* step and the *down* step.

The orientations of the CS planes reported in ref 20 are described by the empirical formula $(hkl) = p(121) + q(011)$, where p and q are integers. When $p/q \geq 1$, which is the case in the measurements reported by Bursill and Hyde,[20] the solutions to the empirical formula correspond to orientations of the CS planes between (132) and (121).

As both the 1×2 reconstruction and the CS plane intersections are essentially one-dimensional structures, they have recently attracted attention as templates for directing the growth of molecular self-assembly structures[13,14] and metal nanoparticles.[16]

In this article, we show that the reduction behavior of the ultrathin titania closely resembles that of the native surface; both the 1×2 reconstruction and CS planes can be seen on the ultrathin TiO_2(110). This is, to our knowledge, the first report of CS planes in TiO_2 ultrathin films, although similar phases have been observed for other, much thicker (300–1000 Å) metal oxide films.[25,26]

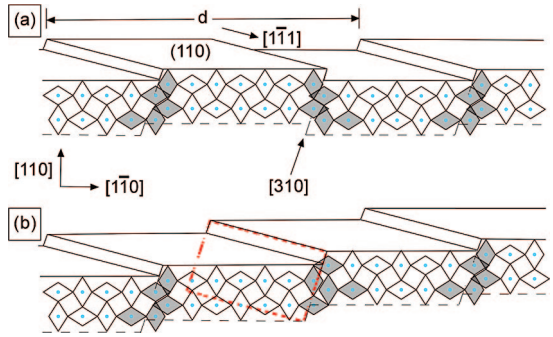

Figure 2. Schematic representation of crystallographic shear planes intersecting the TiO_2(110) surface. Blue circles represent Ti atoms, and rhombi are the cross sections of Ti atoms in pseudo-octahedral co-ordination. Cross sections represent a cut parallel to the (001) plane. CS planes of (132) orientation are indicated by dotted lines intersecting the (001) plane along the [310] direction and by solid lines intersecting the (110) plane along the [1$\bar{1}$1] direction. One of these CS planes is highlighted with a red dashed perimeter. The rhombi which form the CS planes are shaded gray. The CS planes induce half-height steps at the TiO_2(110) surface resulting in (a) an "up–down" half-height step arrangement and (b) a "staircase" half-height step arrangement. The periodicity between the up–down pairs, *d*, is indicated.

RESULTS AND DISCUSSION

The 1×2 Reconstruction. Although the rutile islands are often terminated by the 1×1 phase, more reduced islands are also found. Figure 3 shows STM images of some islands terminated by the TiO_2(110) 1×2 reconstruction. The islands are typically 1–4 atomic layers thick.

The high-resolution image in Figure 3b shows a large density of links present. These links are in the form of cross-links, as well as single links and (elongated) rosette structures. For more reduced 1×2 surfaces, STM images of the native TiO_2(110) crystal reveal the formation of similar links between 1×2 rows.[7–9,11,13,14,16,18] They are known to be mobile upon annealing and to form cross and rosette shapes as well as single links.

Two feasible models have been proposed recently for these links. Bowker et al.[7,9] suggest that a new type of 1×2 "added Ti_3O_6 row" forms and that these rows contain links between them. More recently,[8] a model was proposed for the links which is based on the original added Ti_2O_3 row model described above. At present, it has not been established whether either of these interpretations of the links is correct, but there is a consensus that these structures represent a reduced phase.

A line profile along the TiO_2 [1$\bar{1}$0] direction (Figure 3c) reveals periodic rows every 13.0 Å. These rows are themselves composed of two ridges, separated by 3.4 Å, which is a close match to measurements on the native surface.[8] The apparent corrugation of the 1×2 rows in the present study ranges between 0.5 and 1.7 Å. Presumably, the variation in the corrugation arises from differing tip conditions and possibly also depends on the distance of the TiO_2 surface from the conducting metallic substrate, which varies from island to island.

No areas of the TiO_2(110) 1×2 reconstruction were detected after further annealing of such surfaces to 773 K in 1×10^{-7} mbar O_2, suggesting that the TiO_2 stoichiometry can be restored by further oxidation. This implies that the 1×2 reconstruction is caused by incomplete oxidation of the as-deposited Ti.

Crystallographic Shear Planes. The LEED pattern of the supported titania following annealing to 1110 K is shown in Figure 4, together with a schematic diagram

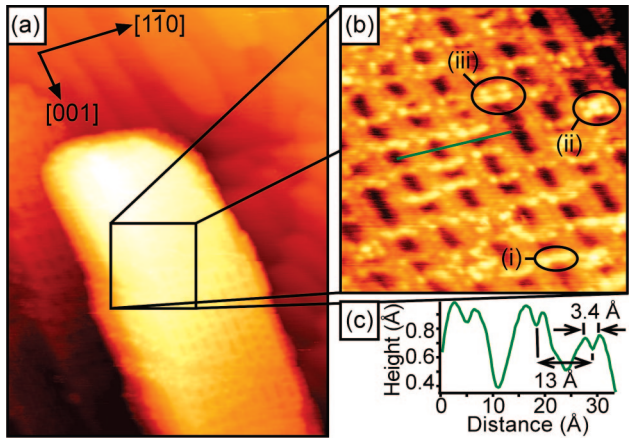

Figure 3. STM images of TiO_2 islands with a 1×2 termination. (a) Large-scale (350 × 470 Å^2, 1.05 V, 3.44 nA) image. (b) High-resolution smoothed image (90 × 90 Å^2, 1.00 V, 1.00 nA). A single link (i), a cross-link (ii), and a rosette link (iii) are indicated, as well as the orientation of TiO_2(110). (c) Line profile along the line drawn in (b).

of the pattern. Discrete spots are observed running along [1$\bar{1}$2] and [$\bar{1}$12]. These spots will be referred to as "⟨112⟩" spots. The ⟨112⟩ spots have a periodicity of about 1/16 of the [1$\bar{1}$2] (or [$\bar{1}$12]) unit vector. This corresponds to a real space distance of ~35 Å, which matches the periodicity of the CS plane up–down pairs observed in our STM images (discussed later) and those taken from the crystallographically sheared native surface.[15]

By considering symmetrically equivalent CS planes, Bennett *et al.*[15] deduced that a CS plane of the {*hkl*} family intersects the (110) plane along $\langle p + q, \overline{p+q}, 3p + q\rangle$ and $\langle \overline{p+q}, p + q, 3p + q\rangle$. The ⟨112⟩ LEED spots described above are therefore consistent with the {132} family of CS planes. In addition, all CS planes intersect the (110) plane along [1$\bar{1}$1] and [$\bar{1}$11], and intersection lines should therefore be observable in STM images oriented at ±65.5° with respect to the TiO_2 [001] azimuth.

Figures 5 and 6 show STM images of the crystallographically sheared film. The morphology of the supported TiO_2 has clearly changed in comparison to the STM image of the rutile islands, shown in Figure 3. Islands can no longer be observed. Instead, continuous films are seen, separated by step edges and facets, which can be up to 50 Å high and 600 Å wide. The average thickness of the crystallographically sheared film is estimated at about four atomic layers.

Regularly spaced lines with a periodicity of ~34–35 Å can be seen along both the terraces and the facets. These lines correspond to intersections of the CS planes with the (110) surface and the facets. On the terraces, line profiles reveal oscillations which are due to an up–down arrangement of CS planes. The periodicity of the up–down pairs is within the range observed for the crystallographically sheared native surface[15,21] and also consistent with the LEED pattern discussed above.

The line profile displayed in Figure 5c shows that the corrugation of the up–down steps is ~1 Å, which is slightly lower than expected for half-steps (1.6 Å). The discrepancy can be explained by the finite size of the tip preventing it from reaching the bottom of the "down" terraces. When this steric restriction of the tip is absent, for example, when there is a half-step leading onto a flat terrace, the apparent height increases to about ~1.3 Å. Furthermore, in higher resolution images, we measure the corrugation of the up–down steps in a range from 1.2 to 1.5 Å. These latter values are in good agreement with the ideal half-height step of 1.6 Å.

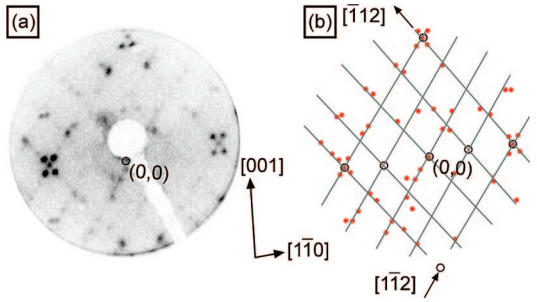

Figure 4. (a) LEED pattern (32 eV) of the crystallographically sheared film. The orientation of TiO_2(110) is indicated. (b) Schematic diagram of (a) drawn to scale. Filled red circles depict the spots present in the LEED pattern. Open circles show the positions of the LEED beams from the TiO_2(110) 1×1 termination. The zero-order spot is labeled. The lines indicate the principal directions of the streaking in the LEED pattern with respect to the TiO_2(110) surface unit cell.

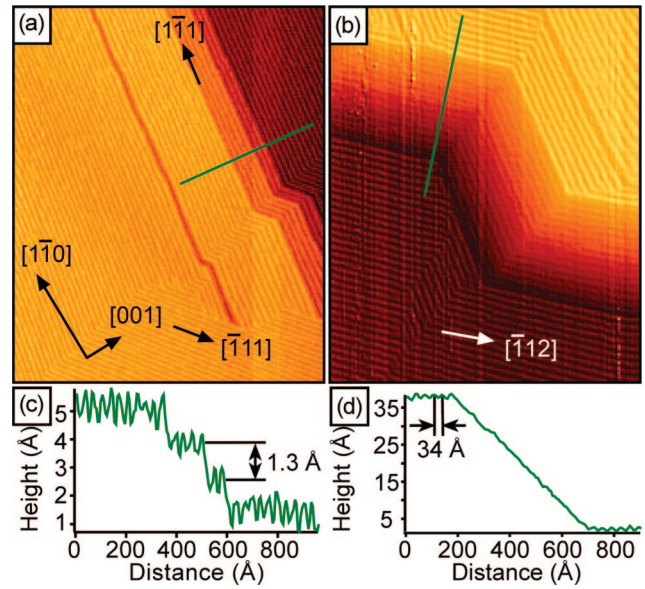

Figure 5. STM images of the crystallographically sheared film: (a) 1700 × 2100 Å^2, 0.30 V, 0.90 nA; (b) 1500 × 1800 Å^2, 0.15 V, 0.80 nA. The arrows indicate both the principal azimuths of the TiO_2(110) surface and the directions of the CS plane intersections at the (110) surface. (c) Line profile along the line indicated in (a). (d) Line profile along the line indicated in (b). The image in (b) has a shadow effect applied, and the line profile in (d) is taken from an image without the shadow applied.

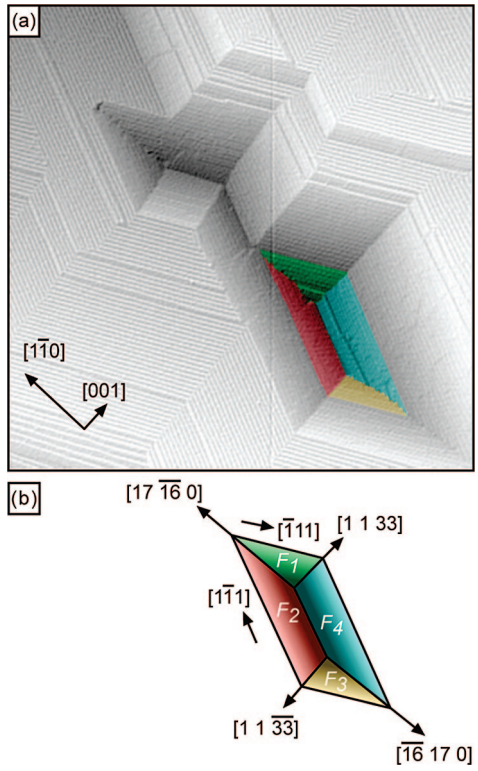

Figure 6. (a) Differentiated STM image of the crystallographically sheared film (3600 × 3600 Å^2, 0.50 V, 4.82 nA). The arrows indicate the principal azimuths of the TiO_2(110) surface. Parts of four facets are highlighted by different colors. (b) Schematic representation of the facet arrangement in the lower part of the STM image, with the same color coding as in (a). F_1, F_2, F_3, and F_4 correspond to the (16 17 $\bar{1}$), (16 17 1), (17 16 1), and (17 16 $\bar{1}$) planes, respectively. The arrows indicate intersections of the facets with each other and with the (110) plane.

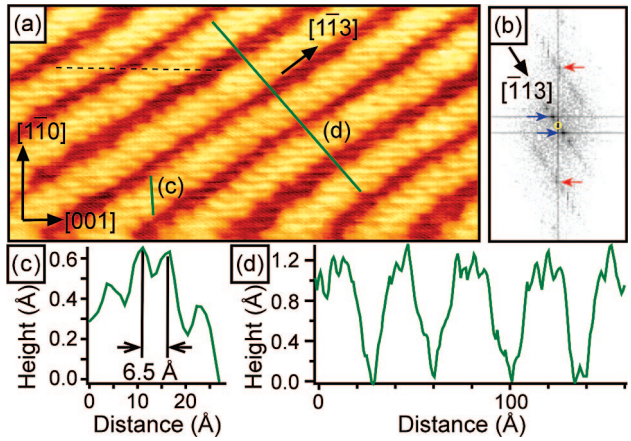

Figure 7. (a) STM image of the crystallographically sheared film (360 × 180 Å^2, 0.15 V, 0.85 nA). The arrows indicate both the principal azimuths of the TiO_2(110) surface and the direction of the CS plane intersections. A dashed guideline shows that the TiO_2(110) 1×1 rows are in-phase across the half-steps. Note that the image in this figure is taken from one of the minority islands with the TiO_2 [001] azimuth oriented parallel to the Ni [001] direction. Similar images were observed on the majority islands, where the TiO_2 [1$\bar{1}$0] azimuth lies parallel to Ni [001]. (b) Fast Fourier transform of the STM image presented in (a). Blue arrows pointing to the right indicate discrete spots arising due to the periodicity of the CS plane up–down pairs, and red arrows pointing to the left indicate the (01) and (0$\bar{1}$) spots of TiO_2(110). An open yellow circle highlights the (00) spot. (c,d) Line profiles along the lines indicated in (a).

An interesting feature of the images in Figures 5 and 6 concerns the step edges. All the step edges are incorporated into the CS shear planes. This is indicated by their alignment parallel to the CS planes and their heights (1.2–1.5 Å), which correspond to half-steps. Bennett *et al.*[15] suggested that step edges would be incorporated into CS planes so that the surface free energy can be reduced by exposing steps of ~1.6 Å instead of the natural 3.25 Å steps. Some of the images of the native surface presented by Bennett *et al.*[15] show this incorporation of step edges with the CS planes.

Further to this, in many cases, such as in the area imaged in Figure 6a, the incorporation of step edges with CS planes causes the film to facet, with (110) terraces separated by CS plane half-steps.

This contrasts with the observations by Murray *et al.*,[11] where the low-index {100}, {111}, and {011} facets were formed on a highly reduced native TiO_2(110) surface. This difference is exemplified by the image in Figure 6, where the facets labeled F_1, F_2, F_3, and F_4 are measured as the (16 17 $\bar{1}$), (16 17 1), (17 16 1) and (17 16 $\bar{1}$) planes, respectively, and are determined by the periodicity of the half-steps. These facets (F_1–F_4) correspond to crystallographically equivalent planes of the rutile structure. The dihedral angle between these facets and the (110) plane is 3.0°, a close match to the 3.7° measured directly from the STM image in Figure 6a. The arrangement of the facets pictured in Figure 6 gives the appearance of oblique wedge-like indentations in the (110) surface.

Such well-defined, wedge-like facets were not observed for the crystallographically sheared native surface. Instead, poorly defined, large-scale faceting was observed in STM, and this was presumed to give the crystal a rippled appearance when viewed by the eye.[15]

A number of the CS planes identified in our STM images were not detected with LEED. This is presumably due to the LEED measurements sampling a different area to the STM. In particular, numerous CS plane intersections are observed in STM images running along [1$\bar{1}$1], [$\bar{1}$11], and [1$\bar{1}$3], the last being indicative of the formation of CS planes of the {121} family.

Figure 7a shows a high-resolution image of a CS plane structure. Here, lines of the CS plane intersections run parallel to the [1$\bar{1}$3] direction, caused by the {121} family of CS planes. The CS plane intersections lead to an up–down arrangement of half-height steps, as discussed previously. The line profile in Figure 7d highlights these up–down steps.

Additional fine structure can be seen in the image, consisting of lines which run in the [001] direction. The separation of these lines along [1$\bar{1}$0] is about 6.5 Å, as shown in the line profile of Figure 7c, indicating that they correspond to the 1×1 rows of the TiO_2(110) surface.

The dashed guideline in Figure 7a is drawn over one of these finer lines. It can be seen that the lines stay in-phase across the half-steps. On the native TiO_2(110) surface, STM images reveal 1×1 rows, which are displaced laterally by half a unit cell in the [1$\bar{1}$0] direction as a single step is crossed.[6] That there is no phase-shift in the 1×1 rows in Figure 7 provides further evidence that the steps are indeed genuine CS plane derived half-steps.

Figure 7b shows a fast Fourier transform (FFT) of the STM image in Figure 7a. The FFT image detects the series of CS plane up–down pairs as an array of spots. The direction in which the spots align corresponds to the direction across which the half-steps run, and the periodicity of the spots matches the separation between pairs of up–down steps and therefore supports our assignment of the analogous LEED ⟨112⟩ spots to periodic CS plane up–down pairs.

In conclusion, we have reported the reduction of Ni(110)-supported TiO_2(110) which forms bulk-like reduced rutile TiO_2(110) structures. STM images show the presence of the oxygen-deficient TiO_2(110) 1×2 reconstruction. Furthermore, we observed the intersections of the {132} and {121} families of CS planes with the (110) surface of the ultrathin film, as previously reported for the native surface. As the CS planes are bulk defects rather than surface defects, we conclude that, structurally, the ultrathin films behave in a bulk-like manner. However, restricting the thickness of the TiO_2(110) in the way described here may confer novel electronic properties which may be useful in applications such as gas-sensing or photocatalysis.

METHODS

STM experiments were carried out in two separate ultra-high-vacuum (UHV) chambers. The 1×2-terminated rutile TiO_2(110) islands were imaged using an Omicron low-temperature STM operated at 77 ± 1 K, with a base pressure of 7×10^{-11} mbar. The CS plane surfaces were characterized using an Omicron variable-temperature STM operated at room temperature and a base pressure of 2×10^{-10} mbar.

The substrate was a single crystal of Ni(110), prepared with cycles of Ar^+ sputtering and vacuum annealing to 1100 K. The cleanliness of the Ni(110) surface was established from sharp (1×1) LEED patterns and the absence of any contaminants in Auger electron spectra (AES). The TiO_2(110) islands were grown on Ni(110) by first depositing Ti by metal vapor deposition (MVD) at room temperature and then oxidizing for 30 min in a pressure of 1×10^{-7} mbar molecular oxygen at a temperature between 873 and 1023 K. The coverage of titanium metal was estimated from AES to be in the range of 2–4 monolayer equivalents (MLE, where 1 MLE corresponds to a coverage of one adsorbate atom per substrate surface unit cell). After oxidizing, rutile TiO_2(110) islands are formed with a thickness between one and four atomic layers, as measured directly with STM. The rutile islands sit on top of an initial wetting layer that is two layers thick. More details of the rutile islands and the wetting layer can be found elsewhere.[1–3]

Crystallographically sheared ultrathin films of TiO_2 have been formed from these Ni(110)-supported TiO_2(110) 1×1 islands by further annealing at 1110 K for 15 min in a pressure of 1×10^{-7} mbar O_2. Similar CS planes could also be formed in the TiO_2(110) ultrathin films by directly annealing the as-deposited Ti to 1100 K for 30 min under a pressure of 1×10^{-7} mbar O_2. STM images were processed using Image SXM v1.81.[27] The thickness of the sheared film (four layers on average) was evaluated from AES in combination with STM measurements of the density and heights of the initially formed rutile islands.

Acknowledgment. We thank Greg Cabailh and Roger Bennett for useful discussions. This work was funded by the EPSRC (UK) and the EU.

REFERENCES AND NOTES

1 Ashworth, T. V.; Thornton, G. Thin Film TiO_2 on Nickel(110): An STM Study. *Thin Solid Films* **2001**, *400*, 43–45.
2 Ashworth, T. V.; Muryn, C. A.; Thornton, G. Nanodots and Other Low-Dimensional Structures of Titanium Oxides. *Nanotechnology* **2005**, *16*, 3041–3044.
3 Papageorgiou, A. C.; Cabailh, G.; Chen, Q.; Resta, A.; Lundgren, E.; Andersen, J. N.; Thornton, G. Growth and Reactivity of Titanium Oxide Ultrathin Films on Ni(110). *J. Phys. Chem. C* **2007**, *111*, 7704–7710.
4 Ashworth, T. V. PhD Thesis, University of Manchester, 2003.
5 Onishi, H.; Iwasawa, Y. Reconstruction of TiO_2(110) Surface: STM Study with Atomic-Scale Resolution. *Surf. Sci.* **1994**, *313*, L783–L789.
6 Diebold, U. The Surface Science of Titanium Dioxide. *Surf. Sci. Rep.* **2003**, *48*, 53–229.
7 Stone, P.; Bennett, R. A.; Bowker, M. Reactive Re-Oxidation of Reduced TiO_2(110) Surfaces Demonstrated by High Temperature STM Movies. *New J. Phys.* **1999**, *1*, 8.
8 Takakusagi, S.; Fukui, K.; Nariyuki, F.; Iwasawa, Y. STM Study on Structures of Two Kinds of Wide Strands Formed on TiO_2(110). *Surf. Sci.* **2003**, *523*, L41–L46.
9 Bennett, R. A.; Stone, P.; Price, N. J.; Bowker, M. Two (1×2) Reconstructions of TiO_2(110): Surface Rearrangement and Reactivity Studied Using Elevated Temperature Scanning Tunneling Microscopy. *Phys. Rev. Lett.* **1999**, *82*, 3831–3834.
10 Blanco-Rey, M.; Abad, J.; Rogero, C.; Mendez, J.; Lopez, M. F.; Martin-Gago, J. A.; de Andres, P. L. Structure of Rutile TiO_2(110)-(1×2): Formation of Ti_2O_3 Quasi-1D Metallic Chains. *Phys. Rev. Lett.* **2006**, *96*, 055502/1–4.
11 Murray, P. W.; Condon, N. G.; Thornton, G. Effect of Stoichiometry on the Structure of TiO_2(110). *Phys. Rev. B* **1995**, *51*, 10989–10997.
12 Pang, C. L.; Haycock, S. A.; Raza, H.; Murray, P. W.; Thornton, G.; Gülseren, O.; James, R.; Bullett, D. W. Added Row Model of TiO_2(110)1×2. *Phys. Rev. B* **1998**, *58*, 1586–1589.
13 Fukui, K.; Sakai, M. Formation of One-Dimensional C_{60} Rows on TiO_2(110)-1×2 and Structural Change of C_{60} Adlayers Induced by Electron Irradiation. *Jpn. J. Appl. Phys., Part 1* **2006**, *45*, 2063–2066.
14 Wang, Y.; Ye, Y.; Wu, K. Adsorption and Assembly of Copper Phthalocyanine on Cross-Linked TiO_2(110)-(1×2) and TiO_2(210). *J. Phys. Chem. B* **2006**, *110*, 17960–17965.
15 Bennett, R. A.; Poulston, S.; Stone, P.; Bowker, M. STM and LEED Observations of the Surface Structure of TiO_2(110) Following Crystallographic Shear Plane Formation. *Phys. Rev. B* **1999**, *59*, 10341–10346.
16 Bennett, R. A.; Newton, M. A.; Smith, R. D.; Evans, J.; Bowker, M. Titania Surface Structures for Directed Growth of Metal Nanoparticles via Metal Vapour Deposition and Metal Organic Chemical Vapour Deposition. *Mater. Sci. Technol.* **2002**, *18*, 710–716.

17 Berkó, A.; Solymosi, F. Study of Clean TiO_2(110) Surface by Scanning Tunneling Microscopy and Spectroscopy. *Langmuir* **1996**, *12*, 1257–1261.

18 Bennett, R. A. The Re-Oxidation of the Substoichiometric TiO_2(110) Surface in the Presence of Crystallographic Shear Planes. *PhysChemComm* **2003**, *3*, 9–14.

19 McCarty, K. F.; Bartelt, N. C. The 1×1/1×2 Phase Transition of the TiO_2(110) Surface—Variation of Transition Temperature with Crystal Composition. *Surf. Sci.* **2003**, *527*, L203–L212.

20 Bursill, L. A.; Hyde, B. G. Crystallographic Shear in the Higher Titanium Oxides: Structure, Texture, Mechanisms and Thermodynamics. *Prog. Solid State Chem.* **1972**, *7*, 177–253.

21 Nörenberg, H.; Briggs, G. A. D. Surface Structure of the Most Oxygen Deficient Magnéli Phase—An STM Study of Ti_4O_7. *Surf. Sci.* **1998**, *402–404*, 738–741.

22 Nörenberg, H.; Tanner, R. E.; Schierbaum, K. D.; Fischer, S.; Briggs, G. A. D. Visualization of Precipitation Induced Crystallographic Shear Planes as One-Dimensional Structures on Surfaces: An STM and RHEED Study on TiO_2(110). *Surf. Sci.* **1998**, *396*, 52–60.

23 Rohrer, G. S.; Henrich, V. E.; Bonnell, D. A. Structure of the Reduced TiO_2(110) Surface Determined by Scanning Tunneling Microscopy. *Science* **1990**, *250*, 1239–1241.

24 Catlow, C. R. A.; James, R. Disorder in TiO_{2-x}. *Proc. R. Soc. London A* **1982**, *384*, 157–173.

25 Li, M.; Altman, E. I.; Posadas, A.; Ahn, C. H. Surface Phase Transitions upon Reduction of Epitaxial WO_3(100) Thin Films. *Thin Solid Films* **2004**, *446*, 238–247.

26 Gao, W.; Altman, E. I. Growth and Structure of Vanadium Oxide on Anatase (101) Terraces. *Surf. Sci.* **2006**, *600*, 2572–2580.

27 Barrett, S. D. http://www.liv.ac.uk/~sdb/ImageSXM.